RSC Advances

PAPER

View Article Online
View Journal | View Issue

Cite this: *RSC Adv.*, 2025, **15**, 5462

Utilization of non-plasticized polymer inclusion membrane for highly selective colorimetric sensor detection of zirconium in environmental samples

Salah M. El-Bahy,[a] Alaa S. Amin, *[b] Refat El-Sayed,[bc] Khaled F. Debbabi,[cd] Nader Hassan[e] and Mai Aish[e]

A pioneering colorimetric optical sensing system utilizing polymer inclusion membranes (PIM) devoid of plasticizers has been innovated for the discerning identification of zirconium(IV) within environmental specimens, characterized by its simplicity, speed, selectivity, and sensitivity. The assembly of this optical sensor relies on a physical immobilization technique, specifically the encapsulation method, which leads to the creation of the sensor membrane. The key components of the PIM sensor include 5-(2-benzothiazolylazo)-8-hydroxyquinolene (BTAHQ) as the reagent, polyvinyl chloride (PVC) serving as the base polymer, and Aliquat 336 functioning as an extractant. Empirical studies reveal that the responsiveness of the optical sensor is significantly affected by diverse parameters including the presence of PVC as the base polymer, thickness of the film, concentrations of BTAHQ and Aliquat 336, temperature, stirring conditions, and the pH level of the aqueous solution. Optimization endeavors have resulted in characterizing the sensor, establishing a linear dynamic range from 4.0 to 110 ng mL^{-1} for Zr(IV), showcasing quantification and detection limits of 3.95 and 1.20 ng mL^{-1}, respectively. The sensor demonstrates a swift response time of absorbance for the PIM-based sensor which is observed at λ_{max} 622 nm. Furthermore, the advanced PIM formulation exhibits stability, and retains its sensitivity, selectivity, and reusability. The method has been successfully applied to determine zirconium in real environmental samples, encompassing soil, water, plant materials, and ore samples.

Received 5th August 2024
Accepted 20th December 2024

DOI: 10.1039/d4ra05674d

rsc.li/rsc-advances

Introduction

In the Earth's crust, the distribution of zirconium is 162 ppm.[1] In 1992, zirconium(IV) minerals production was 808 000 tons in the world. It offers numerous advantageous features, notably its capacity to enhance corrosion resistance, a property highly prized in light of its expanding utilization across various industrial sectors. Zirconium serves as a crucial alloying agent in steels utilized in various applications exposed to corrosive agents. These applications include photoflash bulbs, surgical appliances, lamp filaments, and explosive primers.[2] At reduced temperatures, zirconium demonstrates superconductivity. Consequently, it finds application in producing superconductive magnets, offering potential for widespread electricity generation through direct means.[3] Zirconium alloys have found widespread application as sheathing for nuclear fuel and as core components in water-cooled nuclear reactors. This inclination arises from their low thermal neutron capture cross-section, outstanding corrosion resistance in high-temperature water, and dependable mechanical strength.[4]

The impact of zirconium on biological systems remains a puzzle. While some research proposes a biological impact of zirconium, contrasting studies fail to support this assertion. The low toxicity and high biological inertness of zirconium and its compounds account for their application in the production of medical instruments and implants.[5–8]

Zirconium is broadly used in prostheses, implants and orthodontic applications such as zirconia (ZrO_2). However, according to the previous study, metallic implants degradations result from electrochemical dissolution, frictional wear, or a synergistic combination of the two,[9] which will lead to Zr particles or ions release. The released Zr can migrate systemically,[10] which may lead to cytotoxicity,[11] and bring effects on DNA damage.[12] Although a number of researches have evaluated and proven the availability of Zr implants, the researchers also stressed the urgent need for well-conducted, long-term, randomized controlled trials to establish an evidence-based use of Zr as the reserved promising implant alternative.[13,14]

[a]*Department of Chemistry, Turabah University College, Taif University, Taif, Saudi Arabia*

[b]*Chemistry Department, Faculty of Science, Benha University, Benha, Egypt. E-mail: asamin2005@hotmail.com*

[c]*Department of Chemistry, University College in Al-Jamoum, Umm Al-Qura University, 21955 Makkah, Saudi Arabia*

[d]*Department of Chemistry, Higher Institute of Applied Sciences & Technology of Mahdia, University of Monastir, Tunisia*

[e]*Chemistry Department, Faculty of Science, Port Said University, Port Said, Egypt*

Additionally, sodium zirconium cyclosilicate is useful in treating high levels of potassium in the blood (hyperkalemia).[15] Moreover, chemicals containing zirconium are used in many industrial activities, including refractories that are resistant to heat, ceramics, nuclear reactors, electronic gadgets, and foundry sands.[16] However, chronic exposure to the soluble compounds of zirconium such as zirconium tetrachloride may cause skin and lung granulomas.[17,18] Industrial wastewater can increase the amount of zirconium in the environment. Contaminated soil and water can expose humans to this metal.

Various techniques have been proposed for evaluating zirconium ions, including inductively coupled plasma atomic emission spectrometry (ICP-AES),[19,20] inductively coupled plasma mass spectrometry,[21] X-ray fluorescence spectroscopy,[22,23] inductively coupled plasma-optical emission spectrometry,[24] ultraviolet-visible spectrophotometric methods,[25–30] and laser sampling inductively coupled plasma-optical emission spectrometry.[31] Additional approaches comprise polarography,[32] X-ray fluorescence,[33] ion-selective electrode,[34] neutron activation,[35] high-performance liquid chromatography,[36] voltammetry,[37] chronoamperometry,[38] liquid chromatography,[39] and chelating ion exchange followed by spectrophotometric detection.[40] However, some of these methods require expensive equipment and complex sample preparation steps, which are not suitable for online or field monitoring. Moreover, many of these techniques are costly and demand specialized expertise. Consequently, proposing optical sensors presents an attractive alternative for assessing both inorganic and organic species due to their inherent advantages of simplicity, reliability, speed, cost-effectiveness, and non-destructive nature.

In recent times, there has been a surge in the need for the creation of chemical sensors capable of facilitating easy, simple, rapid, and cost-effective analysis of environmental samples in real-time. In this context, chemical sensors leveraging optical absorption measurements stand out as one of the advancing techniques in the field of analytical chemistry. They have been recognized for their advantageous features, including low-cost manufacturing and the potential for miniaturization, making them highly appealing in the field of analytical chemistry.

Optochemical sensors often rely on immobilizing the reagent through either chemical (covalent bond) or physical (sol–gel, encapsulation, adsorption, *etc.*) techniques, incorporating this sensor design. Immobilization can be accomplished either directly on a suitable material acting as an interface between the sample and the fiber optic system, termed as extrinsic sensors, or on the surface of optical fibers, known as intrinsic sensors.[41–43]

The sensing phase involves immobilizing the reagent within either inorganic or organic materials. The reaction of the analyte alters the absorbance performance of the sensitive layer. In colorimetric determination, metal chromic indicators and organic reagents play a crucial role in designing established sensors.[44] Immobilizing dyes into or onto a solid support is the underlying principle in optical sensing for their application.[45] The ideal immobilization procedures typically involve assembling stable molecules that remain accessible to the dissolving reagent. Two commonly employed methods are physical entrapment[46] and covalent attachment to a functionalized support.[47] Entrapment is technically simpler, but it often results in a longer response time.

For precise analytical applications, membrane-based preconcentration techniques can be customized. To convert a selective membrane of the analyte into an optical chemical sensor (optode), the reagent needs immobilization in a manner responsive to the analyte concentration.[48] The optical sensor membrane is fabricated by embedding the reagent (ionophores, chromoionophores) within a solid matrix, with or without extractant, utilizing highly specialized methodologies.[49–51] These optodes depend on accumulating the analyte on a solid substrate as a chromogenic species, then assessing the absorbance of the solid phase without extracting the chromogenic species. Incorporating extractant improves both the sensitivity and selectivity of optodes compared to solution colorimetry utilizing analogous chromophores.

The main aim of this research was to formulate a specific optical sensor setup for zirconium detection by incorporating 5-(2-benzothiazolylazo)-8-hydroxyquinolene (BTAHQ) within polyvinyl chloride (PVC) as the primary polymer, supplemented with Aliquat 336 as an extractant. The objective was to evaluate their efficiency in spectrophotometric detection of zirconium ions. Scheme 1 represented the chemical structures of Aliquat 336 and BTAHQ as:

Experimental

Instrumentation

A 10 μL microsyringe from Hamilton was employed for dispensing minute reagent volumes into the cell. Spectral

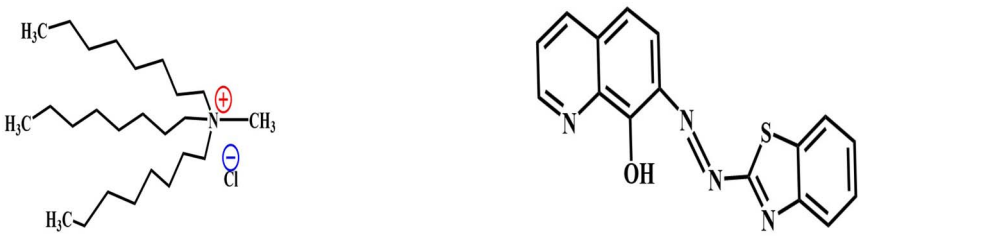

Scheme 1 Representative chemical structures of Aliquat 336 and BTAHQ.

absorption measurements were carried out using a UV-vis spectrophotometer model V 530 by JASCO (Tokyo, Japan). Absorbance readings were acquired by inserting the optical membrane sensor samples (3.0 cm × 1.0 cm) into a quartz cuvette. The obtained absorbance of the optical sensor samples was compared with air and blank sensor samples. To ascertain the solution's pH, a pH meter, specifically the Orion research model 601 A/digital ion analyzer, was utilized. Acceleration of the phase separation process was facilitated by a water bath with precise temperature control and a centrifuge fitted with 10 mL calibrated centrifuge tubes (Superior, Germany). The polymer inclusion membrane (PIM) was prepared as outlined previously,[52] and its characteristics were examined. The thickness of the PIM was evaluated using a digital microscope (Ray Vision Y 103) equipped with a video camera (JVC TK-C 751 EG) and a digital micrometer (Mitutoy, Japan) with an accuracy of ±0.001 mm. Zirconium measurement was conducted using a PerkinElmer (Waltham, MA) model 8300 optima ICP-AES. The operational parameters were adjusted based on the manufacturer's guidelines.

Reagents

All solutions were created using high-purity substances and double-distilled water. Sodium chloride (NaCl), sodium fluoride (NaF), hydrochloric acid (HCl), sodium hydroxide (NaOH), and sulfuric acid (H_2SO_4) solutions (procured from Merck) were prepared by diluting their concentrated solutions accordingly. Triisooctylamine, dinonylnaphtenic sulfonic acid (DNNS), tricaprylylmethyl ammonium chloride (Aliquat-336), 2-nitrophenyloctyl ether (NPOE), dioctyl phthalate (DOP), tris(2-ethylhexyl) phosphate (TEHP), tributyl phosphate (TBP), sodium tetraphenyl borate (NaTPB), and poly(vinyl chloride) [MW 200,000] (PVC) were sourced from Sigma-Aldrich (Steinheim, Switzerland). Tetrahydrofuran (THF), acetic acid (CH_3-COOH), nitric acid (HNO_3), ethanol (EtOH), and dichloromethane (DCM) were acquired from BDH. Additionally, other chemicals utilized were high-purity products.

Standard zirconium solutions (100 μg mL^{-1} and synthetic samples) were created by dissolving $ZrO(NO_3)_2 \cdot 2H_2O$ sourced from Loba Chemie Pvt Ltd, Mumbai, India, in distilled water and standardized following established protocols.[53] Working solutions were derived by a suitable dilution of the stock solution with double-distilled water. Acetate, borate, phosphate, thiel, and universal buffer solutions spanning various pH values of 2.0–12 were prepared according to previously described methods.[54] Stock solutions of interfering ions at 20 000 μg mL^{-1} were prepared by dissolving appropriate amounts of suitable salts in double-distilled water. 5-(2-Benzothiazolylazo)-8-hydroxy-quinolene (BTAHQ) was synthesized following the procedure described earlier.[55,56] The purity was checked by elemental analysis (C, H, N), and spectral studies (IR, and ^{1}H-NMR spectra). In the FTIR spectral band appeared of $\nu_{stretch}$ at 3290 cm^{-1} was corresponded to *o*-OH group and that of $\nu_{stretch}$ 1403 cm^{-1} was corresponded to the –N=N– group. A stock solution of 5.0×10^{-4} M BTAHQ was prepared by dissolving an appropriate amount of pure reagent in a minimal volume of ethanol (15 mL) and then diluted to the desired volume in a 100 mL calibrated flask with ethanol.

Membrane preparation

A unique mixture containing 200 milligrams of Aliquat 336 was concocted in 5.0 milliliters of tetrahydrofuran (THF). A PVC solution was created by dissolving 600 mg of PVC in 10 mL of THF. Following this, both solutions were combined and vigorously stirred to achieve a uniform casting solution for a period of 2.0 hours. The casting solution was then spread onto a flat-bottom Petri dish with a diameter of 9 centimeters, which was subsequently placed on a leveled surface to ensure consistent formation of the polymer inclusion membrane (PIM).

For the purpose of gradual removal of THF from the casting solution, the cover of the Petri dish was shielded with filter paper. After a 48 hours interval to allow for THF evaporation, the clear PIM was cautiously detached from the Petri dish. The PIM was subjected to four washes with double-distilled water. Subsequently, the PIM was submerged and agitated in 25 milliliters of BTAHQ (5×10^{-4} M) for 2.0 hours to achieve uniform coloration. Following this, the PIM underwent an additional pair of rinses with double-distilled water to eliminate any unbound reagents and soluble components, and was then dried using tissue paper folds.

The desiccated PIM was preserved in a sealed airtight plastic bag until further required. Subsequently, the PIM was trimmed to dimensions of 3 centimeters × 1 centimeter, as stipulated for the experiment. Furthermore, the thickness of the PIM was assessed using a digital microscope (Ray Vision Y 103) paired with a video camera (JVC TK-C 751EG). The optical sensor was fabricated by dissolving 600 milligrams of PVC and 200 milligrams of Aliquat 336 in 10 milliliters of THF, employing the identical procedure as that for the control optical sensor comprising PVC and Aliquat 336. The casting solution was then spread onto a flat-bottom Petri dish with a diameter of 9 centimeters and allowed to evaporate for 48 hours, followed by stirring for 2.0 hours.

Absorbance measurement

To evaluate the sensitivity of the Zr(IV)-BTAHQ-Aliquat 336 complex, the absorbance of aqueous Zr(IV) samples was assessed. The sensitivity of the complex relies on the Zr(IV) concentration. Thus, samples containing known quantities of Zr(IV) (volume 25 mL) were created using $ZrO(NO_3)_2 \cdot 2H_2O$. The pH of these sample solutions was regulated to pH 5.25 utilizing the thiel buffering system. At first, a PIM sized at 3 cm × 1 cm was immersed in the Zr(IV) solution spanning concentrations from 0.10–2.75 μg mL^{-1}. Following this, the PIM underwent an additional rinse after being agitated with double-distilled water for 3.0 minutes and was dried using tissue paper folds. The dried PIM was then introduced into the quartz cuvette, and its absorption spectrum was documented. This process was iterated for the remaining Zr(IV) samples. A freshly prepared PIM was employed for each measurement. The absorbance of these samples was registered at 622 nm.

Stoichiometric analysis of the Zr(IV)–BTAHQ complex

The stoichiometry of the resultant complex formed between Zr(IV) and BTAHQ was determined through a comprehensive approach encompassing the molar ratio and the continuous-variation methods (commonly known as Job's method). These methodologies were conducted under the specific conditions of a pH value of 5.25, with both Zr(IV) and BTAHQ concentrations set at 5.0×10^{-3} M. The analysis was executed at the absorption maximum wavelength of 622 nm.

Interferences

To investigate the interferences, the metal cations that were examined consisted of their nitrate and chloride salts. The glassware utilized for manipulating solutions underwent a cleaning process involving the use of a detergent solution, followed by immersion in an aqueous solution of nitric acid (10% v/v), and afterwards rinsed extensively with deionized water on many occasions.

Accuracy and precision assessment

To evaluate the accuracy and precision of the proposed method, six solutions containing varying levels of Zr(IV) ions were analyzed. Repeatability (intra-assay precision) and intermediate precision (inter-assay precision) were determined over six non-consecutive days. These metrics were assessed based on the relative standard deviation (RSD) percentage calculated within the same day and using six replicate measurements obtained through the assay procedure.

Zirconium detection in water

A 5.0 mL water sample underwent treatment with 0.5 mL of a 1.0 M NaOH solution and 0.5 mL of a 0.2 M EDTA solution, if necessary, to eliminate the expected interferences from other metal ions. After thorough mixing, the solution was centrifuged to eliminate any resulting precipitate. Post-centrifugation, each sample of 5.0 mL was adjusted to pH 5.25 using Thiel buffer solutions. Subsequently, these samples were augmented with an appropriate quantity of Zr(IV) and subjected to the membrane procedure as previously outlined.

Zirconium detection in soil

A precisely weighed soil sludge sample was transferred to a 50 mL beaker and subjected to extraction with concentrated HCl (4×5.0 mL). Following neutralization of the extract with dilute NaOH solution, EDTA (5.0%, 5.0 mL) was introduced, if necessary, to avoid the expected interferences from other metal ions. Subsequently, thiel buffer solution of pH 5.25 was added, and the mixture was diluted to 25 mL with water. This resultant solution was then directly employed for Zr detection and color development following the absorbance measurement.

Zirconium detection in plant material

A plant material sample weighing 5.0 g underwent digestion for a duration of 20 minutes with 10 mL of HNO_3. Upon cooling, 0.5 mL of $HClO_4$ was introduced, followed by continued heating for an additional 10 minutes. Subsequent to this step, 10 mL of water and 5.0 mL of HCl were incorporated into the cooled residue. EDTA (5.0%, 5.0 mL) was then added to the solution, if necessary, to complex with other metal ions interfere, which was neutralized with 0.05 M NaOH and diluted to 25 mL. Following that, the solution was adjusted to pH 5.25 in accordance with the absorbance measurement, and it was subsequently subjected to Zr(IV) analysis.

Zirconium detection of in ores

An accurately measured 1.0 gram portion of finely pulverized substance was amalgamated with 5.0 grams of Na_2CO_3 in a porcelain crucible. The mixtures underwent fusion at 1000 °C for a duration of 30 minutes and were dissolved in 5.0 mL of HCl (1 + 1) post-fusion residues. If the solutions displayed cloudiness, filtration was carried out, and the residues on the filters underwent thorough washing. The filtrates and rinses were transferred to a 25 milliliter beaker, with the pH of the final solutions adjusted to 5.25. These combinations were then moved to 100 milliliter measuring flasks and diluted with distilled water to the fill line. Subsequently, these samples were enriched with a suitable quantity of Zr(IV) and subjected to the membrane process as previously outlined.

Zirconium detection using ICP-AES.[19] A portion of the zirconium solution, containing between 0.25 and 45 micrograms of zirconium, was transferred into a 50 milliliter container. The total volume of the metal ion solution was around 30 milliliters. This solution was then passed through a column comprising 1.0 gram of PAN-modified zeolite, after adjusting the solution's pH to 3.5, with a flow rate of 2.0 milliliters per minute. Subsequently, the column was rinsed with 10 milliliters of purified water. The metal ions adsorbed on the column were then eluted with 5.0 milliliters of 2.0 M HCl solution at a flow rate of 1.0 milliliter per minute. The eluate was transferred into a 5.0 milliliter measuring flask. The resultant solution was directly aspirated into the ICP-AES against a blank prepared in the same manner, but devoid of zirconium ions.

Results and discussion

PIM characterization

BTAHQ is often used as a chromgenic reagent for the determination of a number of metals.[55–61] The addition of surfactant-active substances improves the selectivity and sensitivity of the metal determinations due to the batho- and hyperchromic effects that can be observed. In solution; BTAHQ react slowly with Zr(IV) at pH 5.25 using toxic solvent (1,4 dioxane) with long time (60 min) with low absorbance values and at lower wavelength in addition to lack selectivity and interference of a large number of metal ions. In the present work, a colorimetric method for the simultaneous pre-concentration and measurement of Zr(IV) from aqueous samples has been developed using an optical sensor membrane made by a physical incapacitation method, specifically the encapsulation technique, which results

in an optical sensor membrane. The components of the sensitive PIM sensor are Aliquat 336 as an extractant, PVC as the base polymer, and BTAHQ as the colorimetric complexing reagent (sensor). Within a few minutes, the reaction takes place, changing the hue from yellow to violet, which is colorimetrically seen or automatically measured in the absorbance mode.

Initially, the formulated PIM displayed wrinkling, irregularity, and a lack of consistency. However, through revisions to the PIM preparation techniques, a pliable, flexible, consistent, translucent, and self-supporting membrane was attained. Substantial modifications, including adjustments to the membrane composition, maintenance of room temperature at 25 ± 2 degrees Celsius, regulation of room humidity, and extension of the casting solution's evaporation period to 48 hours instead of 24 hours, were identified as crucial for generating superior PIMs. These findings underscore the notable impact of external variables such as temperature and humidity on the PIM fabrication process. Additionally, it was observed that the appearance of the resulting PIM remained unaltered even after storage in a sealed container for one month.

The mean thickness of the fabricated PIM measured approximately 25 ± 5 millimeters. This dimension proves conducive to facilitating the intricate reaction between the reagent and metal ions, while also permitting ion mobility. The membrane's thickness falls within an ideal spectrum, neither excessively thick (>100 mm) nor overly thin (<5 mm), rendering it ideally suited for deployment as a transducer in an optical sensor founded on the co-extraction principle.[62]

Optimization of the PIM-based sensor

In the preliminary stages, multiple permutations of extractants, supportive polymers, and reagents were experimented with to pinpoint the most effective PIM blend for detecting Zr(IV) ions. It was noted that a PIM comprising 75% PVC and 25% Aliquat 336 yielded the most prominent alteration in color and the highest absorbance reading. Therefore, this composition was consistently used in subsequent procedures. The use of DNNS and TiOA resulted in lower absorbance values and longer reaction times. This suggests that the inclusion of Aliquat 336 in the PIM plays a crucial role in generating a novel ternary complex involving Zr(IV)–BTAHQ–Aliquat 336 upon interaction with Zr(IV) ions. The emergence of this ternary complex was substantiated by the bathochromic shift witnessed from 522 to 622 nm in the λ_{max} of the PIM-based sensor, in contrast to the blank sensor prepared under similar conditions but lacking Zr(IV) ions (Fig. 1). The bathochromic shift detected in the λ_{max} spectrum of the Zr(IV)-reagent complex was affected by both the extractant type and the hydrophilicity of the reagent employed. In this investigation, the primary cause of the bathochromic shift was attributed predominantly to the inherent characteristics of BTAHQ and Aliquat 336. BTAHQ comprises negatively charged hydroxyl ions, whereas Aliquat 336 carries positive charges, both of which play pivotal roles in this occurrence. The ion-pairing interaction between these compounds, facilitated by the hydroxyl group's capacity to augment the absorbance of the Zr(IV)–BTAHQ complex, triggers the expulsion of an electron

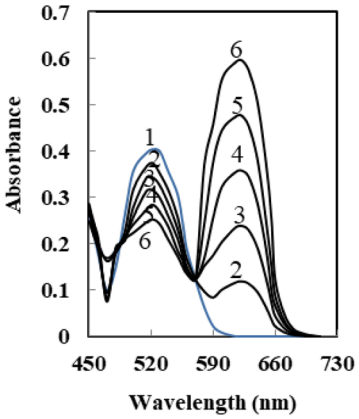

Fig. 1 Absorption spectra of 1- BTAHQ membrane and PIM based sensor upon contact with (2–6), 15, 30, 45, 60, and 75 ng per mL Zr(IV) at pH 5.25.

from the hydroxyl group. This mechanism leads to the deprotonation of the hydroxyl group within the BTAHQ molecule, ultimately contributing to the observed bathochromic shift in the Zr(IV)–BTAHQ–Aliquat 336 ternary complex.

The extractant and polymer's base are the most crucial parameters of PIMs due to their roles in the material's strength and malleability, respectively. Therefore, the concentrations of the extractant and polymer base were altered at three distinct levels, with PIMs containing 75% Aliquat 336 and 25% PVC, essentially no leakage was detected and a rigid membrane was obtained. Because of the minimal quantity of extractant, the PVC filaments are tightly arranged, leading to a strong membrane. The membrane containing 50% Aliquat 336 was flexible, but excessively greasy because of excessive amount of extractant. Additionally, leaching of the reagent was detected. PIMs containing 25% Aliquat 336 and 75% PVC were the most stable and flexible. Table 1 outlines the proportions of Aliquat 336 and PVC and the resultant PIM features for each ratio.

It was established that the peak absorbance was attained when the proportion of Aliquat 336 in the PIM was kept at 25 wt% (m/m). This ratio proved to be ideal for promoting the co-extraction of Zr(IV) ions from the aqueous solution into the PIM, consequently amplifying sensor sensitivity. Nevertheless, incremental increments in the concentration of Aliquat 336 up to 40 wt% (m/m) did not yield any further enhancement in absorbance value (Fig. 2a).

The effect of temperature and room humidity on the sensing performance is studied. The absorption spectra were recorded

Table 1 PIM quality in relation to Aliquat 336 and PVC composition

Conditions PIM	Characteristic
75% Aliquat 336, 25% PVC	- No leakage detected - Rigid membrane
50% Aliquat 336, 50% PVC	- Leaching observed - Oily membrane
25% Aliquat 336, 75% PVC	- Stable, no observed leaching - Flexible

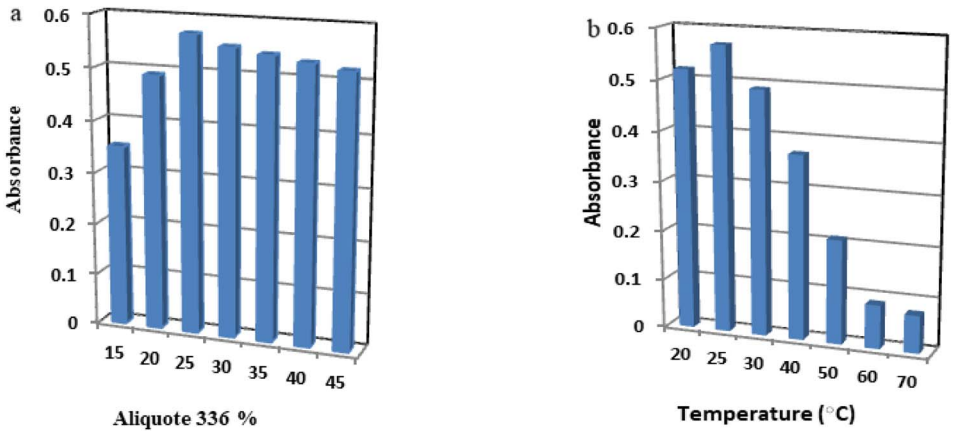

Fig. 2 Effect of (a) Aliquat 336 and (b) temperature on the PIM based sensor immersed in 60 ng mL^{-1} of Zr(IV) at the optimum conditions.

at various temperatures 20 to 50 °C at 622 nm. As the temperature of the Zr(IV) sample increases, the absorbance at 622 nm decreases due to thermal quenching related to the increase of the ions lattice vibrations[63] and the decreasing formation of the complex with the membrane (Fig. 2b). Increasing temperature to $\geq$ 60 °C; there is no variation in absorbance indicating no complex formation between Zr(IV) and BTAHQ. The optimum temperature to achieve highly sensitive and selective results was 25 $\pm$ 2.0 °C.

External stirring of the Zr(IV) solution has a large effect on the response of the formed sensor. About eight fold enhancement was obtained when the Zr(IV) solution was stirred compared with the non-stirred ones. This observation can be explained by the movement of Zr(IV) ions towards the immobilized BTAHQ. The stirring process has accelerated the diffusion of Zr(IV) ions across the membrane to the BTAHQ and consequently expedited the reaction between Zr(IV) ions and BTAHQ. As for the non-stirring process, the diffusion of Zr(IV) ions across the membrane only depends on the concentration gradient.[64]

The selectivity and sensitivity of the Zr(IV) sensor were assessed across various pH values. Different buffer solutions spanning pH 2.5 to 12, including borate, acetate, thiel, phosphate, and universal buffers, were examined, with thiel buffer demonstrating superior effectiveness. Additionally, an optimal pH of 5.25 for the reaction was pinpointed (Fig. 3a). The findings indicated that the inclusion of Aliquat 336 in the PIM did not impact the optimal pH for the formation of the BTAHQ-Zr(IV) complex. The formation of the complex between BTAHQ and Zr(IV) remained achievable within the optimal pH range of 5.0–5.5 in aqueous solution. The findings suggested that the interaction between BTAHQ and Aliquat 336 did not impact the functional groups of BTAHQ crucial for complex formation with Zr(IV). The system's selectivity can be enhanced by varying the pH of the primary phase.[65] Prior to utilizing the membrane, pH studies were conducted using spot tests. Findings indicated that between pH values of 5.0 and 5.5, the complex produced more rapidly than higher pH values. It was noted that absorbance values decreased at both lower and higher pH values. The decline at lower pH values was attributed to the competition between H and Zr(IV) ions for binding with BTAHQ. Conversely, at higher pH values, the formation of $Zr(OH)_4$ in solid form impeded Zr(IV) binding to immobilized BTAHQ.

The efficacy of the optical sensor is impacted not only by the pH value and the method of immobilization for the reaction but also by the type and quantity of the immobilized reagent.[66] In Fig. 3b, the influence of BTAHQ concentration in sensor

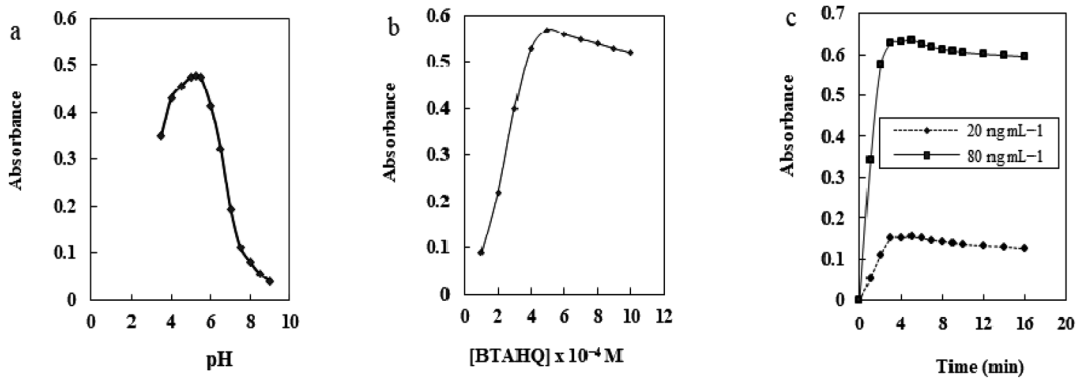

Fig. 3 Effect of (a) pH value, (b) BTAHQ concentration and (c) steady state response time on the sensor response for Zr(IV) at the optimum conditions.

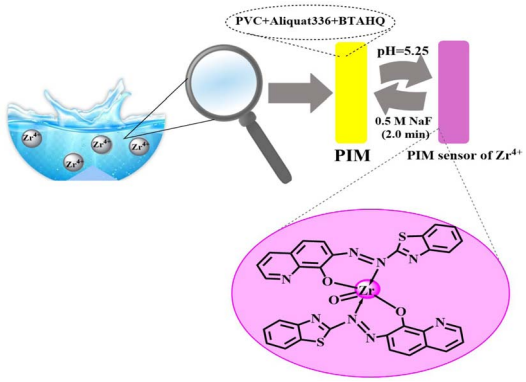

Scheme 2 Schematic representation for the preparation and complexation of Zr(IV) ions on the formed optical sensor.

preparation is illustrated, with a fixed concentration of Zr(IV) (60 ng mL^{-1}) and pH 5.25 for 25 mL. As the initial concentration of BTAHQ rises, the sensor response similarly increases, reaching its peak at a concentration of 5×10^{-4} M. This heightened response can be attributed to the adequacy of this concentration of BTAHQ to react effectively with Zr(IV) ions in the presence of Aliquat 336. However, absorbance exhibited a direct decrease at higher levels due to membrane leakages. The proposed procedure for the complexation between the BTAHQ and Zr(IV) ions is depicted in Scheme 2.

The response time of an optical sensor is primarily dictated by the physical parameters of the sensor setup.[67] The response time of sensors is characterized by the duration it takes for metal ions to diffuse from the solution into the membrane, representing the slowest step in the complexation process. Response time is affected by various factors, including the concentration of Zr(IV) ions controlling their diffusion into the membrane, the reagent loading technique, and membrane thickness. An investigation was carried out to ascertain the optimal response time necessary for the complexation of BTAHQ–Zr(IV). In Fig. 3c, the sensor's response to varying concentrations of Zr(IV) is unveiled. The graph vividly illustrates that the sensor's stable state is intimately tied to the concentration of Zr(IV) ions. Remarkably, the sensor reaches its stable state within three minutes for low Zr(IV) concentrations, while it takes five minutes for higher concentrations. To overcome the challenge of extended response times, a dynamic approach was embraced. Here, the sensor's intensity difference was meticulously noted at a predetermined time, offering a refined method to assess Zr(IV) ion concentration compared to conventional steady-state methods. Following a brief three-minute reaction period, absorbance measurements revealed a substantial signal, underscoring the swift response between BTAHQ and Zr(IV). The reason that the proposed sensor has non first-order kinetics is represented though taking different time to reach the optimum response time. Although reaction that follow first-order kinetics has rate constants that are affected by the concentration of the reactants, the zero-order kinetics have a rate constant and half-life that is independent of the reactants' concentrations. This phenomena is shown and represented in Fig. 3c.

The stoichiometry of the Zr(IV)–BTANQ complex was studied using Job's and the molar ratio procedures. The absorption spectra of BTAHQ and the Zr(IV)–BTAHQ complex were initially recorded and are represented in Fig. 1. The maximum absorption wavelength for BTAHQ was found to be 522 nm, while its complex with Zr(IV) exhibited its peak absorption at 622 nm. Other metal ions has not any absorption band at this wavelength confirming the selectivity of the proposed PIM sensor for Zr(IV) ions. Both methods were subsequently carried out at 622 nm, the wavelength at which the complex demonstrated the highest absorbance. In Job's method, absorbance was plotted against the mole fraction of Zr(IV), with varying concentrations of BTAHQ and Zr(IV) [5×10^{-4} M] keeping the total molar concentration constanted at 1×10^{-4} M. The plot exhibited an inflection point at 0.33, indicating the presence of two BTAHQ molecules in the formed complex. Furthermore, the molar ratio method, the absorbance was plotted against the molar ratio [Zr]/[BTAHQ], yielded a BTAHQ to Zr(IV) ratio of 2.0 (Fig. 4), providing additional evidence for the stoichiometric ratio of (2 : 1) for BTAHQ to Zr(IV). Log K, which is the conditional formation constant, was determined by employing the Harvey and Manning equation with the data obtained from the aforementioned methods. The calculated log K value was detected to be 5.38, while the true constant was found to be 5.20. The interaction between Zr(IV) and BTAHQ leads to the formation of a distinctive violet-colored complex known as the non-ionic complex [Zr(IV)–$(BTAHQ)_2$]. This complex formation is highly specific to Zr(IV) and is widely utilized for the colorimetric determination of Zr(IV) in aqueous samples. This result is confirmed from studying the Fourier-transform infrared spectra (FTIR) for BTAHQ and [Zr(IV)–$(BTANQ)_2]^{2+}$ complex which represented the disappearing of $\nu_{stretch}$ at 3290 cm^{-1} corresponded to o-OH group and shifting of $\nu_{stretch}$ 1403 cm^{-1} corresponded to the –N=N– group to $\nu_{stretch}$ 1394 cm^{-1} after the complexation process. In addition to a new stretching band at 492 corresponding to Zr–O bond formation. The proposed mechanism for the interaction between the BTAHQ sensor and its complexation with Zr(IV) ions is depicted in Scheme 2.

Furthermore, the determination of the stoichiometry of the [Zr(IV)–$(BTAHQ)_2$]: Aliquat 366 ternary complex was conducted

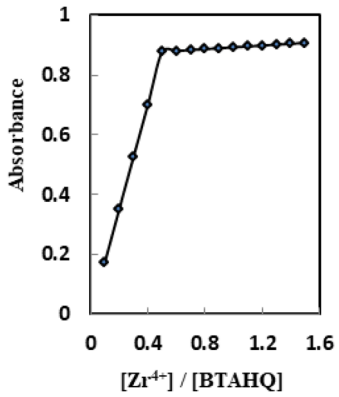

Fig. 4 Molar ratio method for the complexation of Zr^{4+} and BTAHQ ant the optimum conditions.

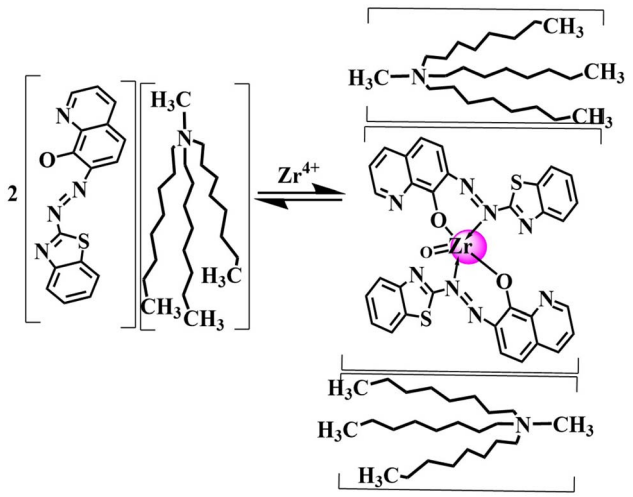

Scheme 3 Representation for the stoichiometric ratio of the formed Zr(IV)–BTAHQ–Aliquat 366 ternary sensor complex.

through Job's and molar ratio methods. It was represented that the maximum absorbance in the molar ratio method is 1 : 2 {[Zr(IV)–$(BTAHQ)_2$]: $(Aliquat\ 366)_2$} while the result from the Job's method is at the mole ratio of 0.35. Both results indicated that the stoichiometric ratio of 1 : 2 {[Zr(IV)–$(BTAHQ)_2$]$(Aliquat\ 366)_2$} is formed. These findings, combined with the infrared (FTIR) spectra of $[Zr(IV)–(BTAHQ)_2]^{2+}$ and the {[Zr(IV)–$(BTAHQ)_2$]$(Aliquat\ 366)_2$} complex, provided the basis for proposing the structural representation of the complex as depicted in Scheme 3. Notably, the conditional formation constant ($\log K$), calculated using Harvey and Manning equation applying the data obtained from the above two methods, was found to be 5.95, whereas the true constant was 5.80. The suggested structure of the complex was postulated as represented in Scheme 3.

The agitation of the Zr(IV) solution exerts a significant influence on the sensor's response. A remarkable eight-fold improvement was noted when the Zr(IV) solution underwent stirring compared to when it remained unstirred. This augmentation can be attributed to the mobilization of Zr(IV) ions toward the immobilized BTAHQ. The stirring process expedites the diffusion of Zr(IV) ions through the PIM, facilitating their interaction with BTAHQ. Conversely, in the absence of stirring, the diffusion of Zr(IV) ions through the PIM relies solely on the concentration gradient.[64]

Assessing the reproducibility and repeatability of the sensor is pivotal in the advancement of chemical sensing technology.[68] These metrics gauge the sensor's consistency and its capability to deliver precise and dependable results, even across diverse batches of manufactured sensors. Reproducibility and repeatability assessments were conducted through four independent trials at varying concentrations of Zr(IV), both in its pure form and in spiked real samples, to validate the reliability and utility of the proposed methodology. Table 2 presents the inter- and intra-day findings across different sample concentrations. The minimal relative standard deviations underscore the dependable repeatability of the optical sensors, proving effective in discerning zirconium ions in both pure and aqueous samples. The observed variance could be attributed to discrepancies in construction variables, including the concentration of immobilized BTAHQ and the thickness of the PIM.

To ensure the membrane sensor's readiness for subsequent measurements, regeneration with an appropriate solution is imperative. Various compounds, including H_2SO_4, HNO_3, H_3PO_4, NaCl, NaF, and EDTA, each at a concentration of 0.5 M, were evaluated for this purpose. The optical sensor was immersed in a Zr(IV) ion solution with a concentration of 60 ng mL^{-1} to establish equilibrium during this assessment. Subsequently, the membrane was immersed in the regenerating solution until the membrane's absorption stabilized. Among the tested reagents, sodium fluoride acid emerged as the most effective. The optimal regeneration time for a 0.5 M NaF solution was determined to be 2.0 minutes as shown in Scheme 2. Consequently, we opted for this specific concentration of NaF and a regeneration time of 2.0 minutes for subsequent procedures. The outcomes revealed complete reversibility of the sensor, with an average regeneration time of about two minutes (Fig. 5). Furthermore, the reproducibility of the sensor post-regeneration was confirmed. At higher concentrations of fluoride, the formation of ZrF_4, is mainly responsible for the interference in pH 5.25 medium, as recorded in the following equation:

Table 2 Inter and intra days precision of the zirconium sensor in pure and spiked water samples, $n = 4$ at 95% confidence level

		Found, ng mL^{-1}		Recovery %		RSD%	
Sample	Taken, ng mL^{-1}	Inter day	Intra day	Inter day	Intra day	Inter day	Intra day
Pure	30	29.65	30.25	98.83	100.83	0.85	0.76
	60	60.40	59.60	100.67	99.33	0.92	1.05
	90	90.75	90.90	100.83	101.00	1.11	1.27
River water 1	25	25.50	25.60	102.00	102.40	1.45	1.32
	50	49.30	50.75	98.60	101.50	1.17	1.25
	75	76.00	74.25	101.33	99.00	1.35	1.47
Industrial waste water	20	20.40	20.30	102.00	101.50	1.22	1.08
	40	39.50	40.65	98.75	101.63	1.50	1.39
	80	81.00	79.20	101.25	99.00	1.27	1.44
Plant material	35	35.75	35.55	102.14	101.57	1.33	1.55
	70	69.55	70.75	99.36	101.07	1.45	1.63
	105	106.25	106.50	101.19	101.43	1.60	1.75

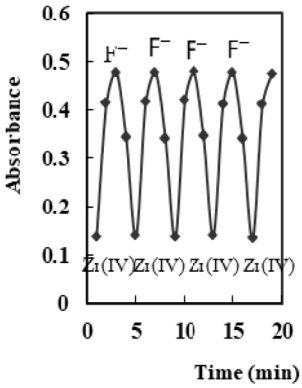

Fig. 5 Reversibility of the sensor treated with 60 ng per mL Zr(IV) and 0.5 M NaF.

$$Zr(BTAHQ)_2 + 4NaF^- \rightleftarrows ZrF_4 + 2BTAHQ$$

Reproducibility was assessed through three regeneration cycles, resulting in consistent outcomes with a relative standard deviation (RSD) of 3.15%. The sensor's regenerative capacity is primarily ascribed to BTAHQ. The hydroxyl groups present in the BTAHQ molecule are anticipated to mitigate leaching concerns. Moreover, as a lipophilic compound, BTAHQ can impede its own release into the aqueous analyte solution. Additionally, the presence of Aliquat 336, functioning as an extractant, effectively confines BTAHQ within the PIM, minimizing the risk of leaching even after multiple regeneration cycles.

The sensor's stability was evaluated by submerging it in an equilibrating solution with a pH of 5.25 for 10 days. Throughout this period, the sensor maintained its stability and demonstrated optimal absorbance at pH 5.25, with a relative standard deviation (RSD) estimated at 1.73%. These findings suggest that the sensor's sensitivity remained unchanged despite exposure to the air atmosphere and equilibrating solution. This stability can be credited to the presence of Aliquat 336 in the sensor, which serves to bind the sensor's components, ensuring both chemical and physical stability.

Interferences

An extensive examination was undertaken to evaluate the impact of foreign ions on the selectivity of Zr(IV) detection, with the objective of identifying the maximum concentration at which interference occurs. Natural water, renowned for its complexity, harbors a diverse array of cations and anions that could potentially disrupt the detection process. Table 3 displays the results for 13 common species typically present in water samples. In this investigation, a tolerance threshold for interfering species was established, ensuring that concentrations causing no more than a 5.0% alteration in the absorbance of a 60 ng per mL Zr solution were deemed acceptable. The table also outlines the boundaries of interfering ions assessed for Zr(IV) detection. The methodology exhibited outstanding selectivity, showcasing superior tolerance for these chemical species with no noteworthy interference observed. Considering that the maximum permissible concentration of these species in water fell below the identified tolerance threshold, the methodology proves to be advantageous for Zr detection in water samples. Although lanthanide ions have the similar physicochemical properties as zirconium, there were no reaction between the studied BTAHQ PIM sensor with them at the optimum reaction conditions reported for Zr(IV) ions.

Table 3 Tolerance limits of several ions for the recovery of 60 ng per mL Zr(IV) [results giving ≤5.0% error]

Species	Tolerance limit mass ratio
Na^+, K^+, Cl^-, $C_2O_4^{2-}$, PO_4^{3+}	12 000
Ca^{2+}, Mg^{2+}, Mn^{2+}, succinate	8000
V^{4+}, Cr^{3+}, Cr^{6+}, NH_4^+, NO_3^-	6000
Fe^{3+}, Cu^{2+}, Zn^{2+}, Br^-, SO_4^{2-}	4500
Tl^+, Be^{2+}, Hg^{2+}, Zn^{2+}, UO_2^{2+}	3000
Cr^{3+}, Pb^{2+}, Al^{3+}, Ni^{2+}	2250
Cs^+, Ag^+, Li^+, CH_3COO^-	1500
Co^{2+}, Mo^{6+}, IO_3^-	1000
La^{3+}, Sc^{3+}, Y^{3+}	750
Ti^{4+}, Hf^{4+}, Th^{4+}	500

The discriminatory capacity of the colorimetric-based sensor is governed by various factors, encompassing the pH level of the reaction, wavelength choice, the chemical composition of the reagent, and the impact of immobilization. Each interaction between metal and reagent attains its peak efficacy at a distinct pH value. Through this investigation, the sensing reaction displayed its utmost efficiency at pH 5.25, yielding maximal absorbance values. Conversely, disparate metal ions showcased their peak intensities at varying pH levels. This underscores the significance of fine-tuning reaction parameters to attain selective and precise detection of the desired analyte.

Analytical characteristics

The developed sensor exhibits a linear dynamic range for Zr(IV) ion concentration spanning from 4.0 to 110 ng mL^{-1} (refer to Table 4). The corresponding correlation equation is encapsulated by the elegant expression $Y = 7.95X - 0.11$ ($R^2 = 0.9988$, $R = 0.9994$), where Y represents absorbance, and X signifies the Zr(IV) ion concentration (M). These quantification and detection limits are defined as LOQ = 10SB/m and LOD = 3SB/m, where LOQ, LOD, SB, and m represent the quantification limit, detection limit, standard deviation of the blank, and slope of the calibration graph, respectively.[69] The calculated LOQ and LOD limits estimated as 3.95 and 1.2 ng mL^{-1}, respectively (Table 4). Remarkably, the achieved LOD[69] is notably lower than those documented in prior studies[11,70–84] (Table 5). This enhancement can be attributed to the inclusion of Aliquat 336 in the PIM, which bolsters the extraction of Zr(IV) ions from the aqueous phase, thereby augmenting sensor sensitivity. The linear range (Fig. 6) and detection limit of the developed sensor are deemed satisfactory compared to existing methods. However, an examination of the literature revealed a scarcity of reports on optical sensors employing chip reagents for Zr(IV) ion assessment. Nevertheless, the sensor exhibits commendable

Table 4 Analytical features of the proposed method

Parameters	PIM method	Parameters	PIM method
pH	5.25	Regression equation	
Beer's range (ng mL^{-1})	4.0–110	Slope (μg mL^{-1})	7.75
Ringbom range (ng mL^{-1})	10–105	Intercept	−0.11
Molar absorptivity (L mol^{-1} cm^{-1})	7.33 × 106	Correlation coefficient (r)	0.9994
Sandell sensitivity (ng cm^{-2})	0.007	RSD (%)	1.75
Detection limit (ng mL^{-1})	1.20	Quantification limit (ng mL^{-1})	3.95

Table 5 Comparative analysis of various reagents for spectrophotometric determination of zirconium with published methods

Reagents	λ_{max} (nm)	ε (L mol^{-1} cm^{-1})	LOD (μg L^{-1})	Remarks	Ref.
Aresnazo III	665	1.50×10^4		Uranium is interfere	70
Arsenazo III	—	—	0.48	SPE required	71
Arsenazo III	665	1.54×10^4	50	Al^{3+}, Th^{4+}, Fe^{3+} interfere	72
Janus green dye	606	—	80	Catalytic oxidation by BrO_3^-	73
Xylenol orange	429	6.90×10^5	120	Extraction with hexane	74
4-(2-Pyridylazo)-resorcinol	530	6.60×10^4	200	Uranium is interfere	65 and 76
Alizarin res S	520	7.04×10^3	100	Heating required	77
Chrome azurol S	598	3.93×10^3	242	Extraction is not required, uranium is not interfere	78
Xylenol orange	551	3.5×10^3	700	F^-, Fe^{3+} interfere	79
Xylenol orange, and cetyltri-methylammonium bromide	592	—	10	Fe^{3+} interfere	80
2-(6-Bromo-2-benzothiazo- lylazo)-5-diethylaminophenol	420	4.40×10^5	30	Extraction required	25
2-(5-Bromo-2-pyridylazo) -5-diethylaminophenol	585	1.54×10^5	60	Methanol–water mixture	81
5,7-Dibromo-8-hydroxy quinoline	416	1.05×10^4	600	Extracted with $CHCl_3$	82
2-(2-Benzothiazolylazo)-3-hydroxyphenol	569	6.38×10^6	1.25	Solid phase spectra	83
2-Amino-4-(3-chlorophenyl-azo) pyridine-3-ol	569	—	7.2	Optical sensor	84
BTAHQ	656	7.33×10^6	0.20	Optical sensor	PM[a]

[a] PM: the proposed method.

sensitivity relative to alternative techniques for Zr(IV) ion detection.

The absorbance values were measured at various concentrations of Zr(IV) in order to identify the concentration range in which Beer's law is valid. The range of 4.0–110 ng mL^{-1} was followed when following the Beer's plot as described in the above absorbance measurement section. As a result, the Ringbom plot[85] between log C of Zr(IV) and (1/T) where 'T' is the transmittance was estimated. The plot has a sigmoid shape with a linear segment at concentration values between 10 and 105 ng mL^{-1}; hence, it is considered the ideal operating range. Additionally, the lowest concentration in (μg mL^{-1}), according to molar absorptivity calculated as the slope of calibration curve when the [Zr(IV)] in molarity, and Sandell's sensitivity (or index),[86] yields an absorbance of 0.001 across a 1.0 cm path length.

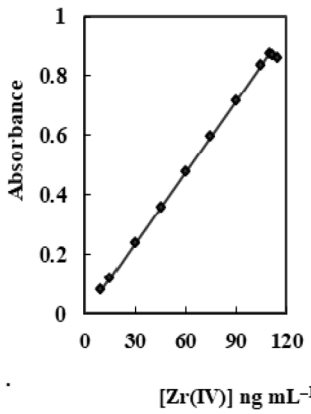

Fig. 6 Calibration curve for Zr(IV) using the proposed PIM sensor at the optimum conditions.

The suggested sensor outperforms various analytical methods, as indicated in Table 6. It showcases remarkable selectivity alongside lower detection and quantification limits. Additionally, it boasts several advantages regarding sensitivity and tolerance to interference. To our knowledge, this marks the inaugural application of BTAHQ as a chromophoric reagent for preconcentration in a PIM sensor designed for Zr(IV) ion detection.

Optode precision, accuracy, and durability

To assess reproducibility, six membranes were individually fabricated under identical conditions, and their absorbance responses were measured in a 60 μg per mL Zr(IV) ion solution. The relative standard deviation (RSD) for the responses among the optodes was found to be 1.95%. Precision was further

Table 6 Comparative data from previously reported techniques for zirconium determination

Ligand/adsorbent	Measurement technique	Sample (mL)	Enrichment factor	LOD (ng mL^{-1})	RSD (%)	Ref.
Dibenzoylmethane (DBM)-Triton X-114	ICP-OES	50	37.0–43.6	15	6.1	24
Quinalizarine – triton X-114	ICP-OES	100	38.9	0.26	2.9	19
8-Hydroxyquinoline/vinyl polymer resin	ICP-MS	250	50	0.15	2–4	88
Surface imprinted amino-functionalized silica gel	ICP-AES	400	200	0.14	1.49	89
Arsenazo-III	ICP-AES	100	250	1.0	1.0–2.5	90
Quinalizarin/octadecyl silica-polyethylene	ICP-AES	25	330	40	1.6	20
2-(2-Benzothiazolylazo)-3-hydroxyphenol						
5-Br-PADAP	UV-vis	150	100	0.2	4.3	91
2-(5-Bromo-2-pyridylazo)-5-diethylamino-phenol	RP-LC	100	—	0.2	4.3	39
(5-Br-PADAP)						
PAN/HDTMA-Br coated clinoptilolite	ICP-AES	50	130	0.1	0.9–2.3	20
2-(2-Benzothiazolylazo)-3-hydroxyphenol	UV-vis	100	—	1.25	1.34	83
BTAHQ			—	0.2	1.25	PM

evaluated by exposing the optodes to 60 and 100 ng per mL Zr(IV) ion solutions under optimal conditions, with measurements taken on the same day (intra-day precision, $n = 6$) and over three consecutive days (inter-day precision, $n = 6$). The precision results were reported as % RSD, with intra-day values of 2.25% and 1.80%, and inter-day values of 2.05% and 1.90%, respectively. Accuracy was tested by recovering known concentrations of Zr(IV) ions (30, 60, 100 ng mL^{-1}) in six replicates. The recovery percentages obtained were 97.25%, 102.67%, and 98.20%, respectively, demonstrating a close match between the actual and measured values. Additionally, the optodes operational lifespan was evaluated using two different methods.

In the first approach, the sensor's lifespan was evaluated by repeatedly immersing a single membrane in a 60 ng per mL Zr(IV) solution under optimal conditions. After 35 measurements, a slight decrease of approximately 4.2% in absorbance intensity was noted. Additionally, a separate membrane was submerged in water for a maximum duration of one month. After this period, the absorbance at 622 nm decreased by 4.8%. These findings

Table 7 Zirconium recovery experiments in real Zr-free water samples spiked with known amounts of zirconium

Sample	Added (μg L^{-1})	Found[a] (μg L^{-1})		Recovery (%)	t-Test[b]	F-Value[c]
		PM	ICP-AES			
Tap water	—	—	—			
	25	24.80	25.40	99.20	1.11	
	50	50.75	51.10	101.50		2.57
River water 1	—	—	—			
	40	40.50	39.40	101.25	1.27	
	80	81.00	79.20	101.25		2.61
River water 2	—	—	—			
	50	50.50	49.20	101.00	1.65	
	100	98.20	102.30	98.20		3.38
Industrial waste water	—	—	—			
	30	29.70	30.40	99.00	1.42	
	60	60.75	61.00	101.25		2.88
Polluted water	—	—	—			
	35	35.50	29.60	101.43	1.33	
	70	69.15	71.00	98.79		2.76
Red sea water	—	—	—			
	45	44.40	45.75	98.67	1.72	
	90	91.00	88.80	101.11		3.55
Mediterranean sea water	—	—	—			
	20	20.30	19.60	101.50	1.54	
	40	39.50	40.90	98.75		3.28

[a] The measured amounts are the average of six determinations. [b] Tabulated t-value for five degrees of freedom at P (0.95) is 2.57. [c] Tabulated F-value for five degrees of freedom at P (0.95) is 5.05.

Table 8 Typical zirconium recovery experiments in real Zr-free plant, soil and stone samples spiked with known amounts of zirconium

Sample	Added (μg L^{-1})	Found[a] (μg L^{-1})		Recovery (%)	*t*-Test[b]	*F*-Value[c]
		PM	ICP-AES			
Plant material (5.0 g cabbage)	20	20.15	19.75	100.75	1.52	
	40	40.25	39.60	100.63		3.19
	60	59.50	60.90	99.17	1.82	
	80	79.10	81.20	98.88		2.32
Soil sludge (1.0 g)	25	24.80	25.50	99.20	1.08	
	50	50.75	49.10	101.50		2.87
	75	74.25	76.20	99.00	1.56	
	100	98.80	102.20	98.80		3.05
Clay stone (μg g^{-1})	30	30.60	30.50	102.00	1.47	
	60	61.00	61.30	101.67		3.23
	90	88.80	91.50	98.67	1.67	
	110	111.00	107.80	100.91		2.89
Iron stone (μg g^{-1})	17.5	17.60	17.35	100.57	1.43	
	35	35.50	34.25	101.43		2.77
	70	69.30	71.00	99.00	1.84	
	105	103.75	107.00	98.81		3.46

[a] The measured amounts are the average of six determinations. [b] Tabulated *t*-value for five degrees of freedom at *P* (0.95) is 2.57. [c] Tabulated *F*-value for five degrees of freedom at *P* (0.95) is 5.05.

indicate that the sensor exhibits excellent stability, maintaining its performance even with extended use and storage, confirming its reliability for multiple applications and a minimum storage period of one month.

Analytical applications

The practical utility of the developed sensor was evaluated by testing various spiked samples. These samples comprised river water, tap water, sea water, polluted water, and industrial waste water, into which small aliquots (a few microliters) of a Zr(IV) solution were added. This assessment aimed to determine the impact of the sample matrix and interfering ions on the response of the optical sensor. The results presented in Table 7 demonstrate a satisfactory agreement between the added and measured zirconium concentrations, underscoring the sensor's efficacy for routine measurements.

To gauge the analytical applicability of the developed optical sensor, zirconium levels in plant, soil, and stone samples were examined. Three types of samples, namely cabbage, sludge, and iron and clay stones, were chosen for this purpose. The results obtained from this procedure are summarized in Table 8. It is observed that the mean recoveries for different concentrations of added Zr(IV) in the samples fall within the range of 98.67% to 102.00%. Hence, the proposed sensor showcases successful applicability for determining Zr(IV) levels in real samples.

The efficacy of the proposed sensor was assessed by calculating the *t*-value for accuracy and conducting an *F*-test for precision, comparing it with the ICP-AES method. Mean values were obtained and subjected to Student's *t*-test and *F*-test at a 95% confidence level with five degrees of freedom.[87] The results revealed that the obtained values (Tables 7 and 8) did not exceed the theoretical ones. The broader range of determination, enhanced accuracy, increased stability, and reduced time consumption underscore the advantages of the proposed technique over alternative methods.

Conclusion

A pioneering optical sensor was engineered for the detection of zirconium ions. In this innovative approach, a PVC sensing film, boasting enhanced optical and mechanical attributes, acted as a base for immobilizing BTAHQ. The membrane showcased a reversible shift in color, transitioning from orange to violet upon exposure to Zr(IV) ions. The operational scope was broadened to encompass concentrations ranging from 4.0 to 110 ng mL^{-1} of Zr(IV) ions, with a detection limit as low as 1.20 ng mL^{-1}. Notably, the sensor exhibited a rapid response time of under 3.0 minutes for 60 ng per mL Zr(IV) ions. Comparison with previously described methods for Zr(IV) detection reveals that the developed sensor, besides its rapidity and simplicity, offers a detection limit comparable to many other techniques. The sensor could be easily regenerated using 0.5 M of F^- and exhibited full reversibility. Ultimately, the fabricated optical sensor proved successful for monitoring Zr(IV) in real water and biological samples.

Data availability

The authors declare that the data supporting the findings of this study are available within the article.

Author contributions

Salah El-Bahy and Nader Hassan: conceptualization, investigation, data curation, visualization, methodology, validation, writing – original draft, writing – review & editing. Refat El-Sayed and Khaled Debbabi: data curation, conceptualization,

methodology, validation, investigation, visuali-zation, writing – original draft & editing. Alaa Amin: conceptualization, supervision, validation, methodology, investigation, writing – original draft, writing – review & editing.

Conflicts of interest

The authors declare that they have no known competing financial interests or personal relationships that could have appeared to influence the work reported in this paper.

Acknowledgements

This research was funded by Taif University, Saudi Arabia. Project No. (TU-DSPP-2024-20). The authors extend their appreciation to Taif University, Saudi Arabia for supporting this work through project number (TU-DSPP-2024-20).

References

1 J. D. Lee, *Concise Inorganic Chemistry*, Chapman & Hall, London, 1996, 5th edn, p. 684.
2 A. Varghese and L. George, *Spectrochim. Acta, Part A*, 2012, **95**, 46–52.
3 J. B. Hedrick, *U.S. Geological Survey Minerals Yearbook*, 2000, p. 87.
4 N. Ni, S. Lozano-Perez, J. Sykes and C. Grovenor, *Ultramicroscopy*, 2011, **111**, 123–130.
5 M. R. Katunar, A. G. Sanchez, A. S. Coquillat, A. Civantos, E. M. Campos, J. Ballarre, T. Vico, M. Baca, V. Ramos and S. Cere, *Mater. Sci. Eng., C*, 2017, **75**, 957–968.
6 S. Sequeira, M. H. Fernandes, N. Neves and M. M. Almeida, *Int*, 2017, **43**, 693–703.
7 S. Ghosh, A. Sharma and G. Talukder, *Biol. Trace Elem. Res.*, 1992, **35**, 247.
8 D. B. N. Lee, M. Roberts, C. G. Bluchel and R. A. Odell, *ASAIO J.*, 2010, **56**, 550–556.
9 M. J. Yaszemski, D. J. Trantolo, K. U. Lewandrowski, V. Hasirci, D. E. Atobelli and D. L. Wise, *Biomaterials in Orthopedics*, CRC Press, USA, 2003, p. 63.
10 D. Olmedo, M. B. Guglielmotti and R. L. Cabrini, *J. Mater. Sci.:Mater. Med.*, 2002, **13**, 793–796.
11 Y. Chen, S. Roohani-Esfahani, Z. Lu, H. Zreiqat and C. R. Dunstan, *PLoS One*, 2015, **10**, e0113426.
12 M. Caicedo, J. J. Jacobs, A. Reddy and N. J. Hallab, *J. Biomed. Mater. Res., Part A*, 2008, **86A**, 905–913.
13 R. B. Osman and M. V. Swain, *Materials*, 2015, **8**, 932–958.
14 R. Depprich, C. Naujoks, M. Ommerborn, F. Schwarz, N. R. Kubler and J. Handschel, *Clin. Implant Dent. Relat. Res.*, 2014, **16**, 124–137.
15 M. Nagard, B. Singh and D. W. Boulton, *Clin. Kidney J.*, 2021, **14**, 1924–1931.
16 L. Xu, Y. Xiao, A. van Sandwijk, Q. Xu and Y. Yang, *Energy Mater.*, 2014, 451–457.
17 H. Faghihian and M. Kabiri-Tadi, *Microchim. Acta*, 2010, **168**, 147–152.
18 Agency for Toxic Substances and Disease Registry, *Toxicological Profile for Polychlorinated Biphenyls*, Agency for Toxic Substances and Disease Registry, Atlanta, GA, 2000, available: **http://www.atsdr.cdc.gov/toxprofiles/tp17.html**, accessed 6 October 2006.
19 H. Karami, M. F. Mousavi, Y. Yamini and M. Shamsipur, *Microchim. Acta*, 2006, **154**, 221–228.
20 H. Faghihian and M. K. Tadi, *Microchim. Acta*, 2010, **168**, 147–152.
21 S. Tian, F. Moynier, E. C. Inglis, N. K. Jensen, Z. Deng, M. Schiller and M. Bizzarro, *J. Anal. At. Spectrom.*, 2022, **37**, 656–662.
22 D. V. Vivit and B. S. W. King, *Geostand. Geoanal. Res.*, 2007, **12**, 363–370.
23 Y. V. Kuminova, V. A. Filichkina, M. N. Filippov and A. S. Kozlov, *Inorg. Mater.*, 2023, **59**, 1470–1473.
24 S. Shariati, Y. Yamini and M. K. Zanjani, *J. Hazard. Mater.*, 2008, **156**, 583–590.
25 C. P. Zhang, D. Y. Qi and T. Z. Zhoum, *Talanta*, 1982, **29**, 1119–1121.
26 R. P. Larsen, L. E. Ross and G. Kesser, *Talanta*, 1960, **4**, 108–114.
27 R. El-Sheikh, E. M. El-Sheikh, M. S. Khalafalla, L. I. Mahfouz, M. M. El-Gabry, A. A. Gouda and I. J. Envir, *Anal. Chem.*, 2023, **103**, 4225–4238.
28 T. Prathibha, B. R. Selvan, V. Hemalatha, M. A. Suba, S. Chandra, D. Shaji, S. K. Vijay, K. Sundararajan and N. Ramanathan, *J. Radioanal. Nucl. Chem.*, 2022, **331**, 2383–2391.
29 E. Zolfonoun, *Anal. Methods Environ. Chem. J.*, 2020, **27**, 18–24.
30 W. H. El-Shwiniy, S. I. El-Desoky, A. Alrabie and B. Abd-El-wahaab, *Spectrochim. Acta, Part A*, 2022, **279**, 121400.
31 S. Lin, C. Peng and J. Anal, *J. Anal. At. Spectrom.*, 1990, **5**, 509–514.
32 J. Tursunqulov, N. Qutlimurotova, M. Fayzullayeva, E. Berdimurodov, S. Raximov, Z. Smanova, A. Dadamatov, N. Aliev, A. Hosseini-Bandegharaei and I. J. Envir, *Anal. Chem.*, 2024, **31**, 1–24.
33 Y. V. Kuminova, V. A. Filichkinaa, M. N. Filippov and A. S. Kozlov, *Inorg. Mater.*, 2023, **59**, 1470–1473.
34 G. G. Mohamed, H. A. Mohamed and E. Y. Fraga, *Microchem. J.*, 2020, **157**, 105063.
35 T. V. Rebagay and W. D. Ehmann, *J. Radioanal. Chem.*, 1970, **5**, 51–60.
36 S. J. J. Tsai and H. T. Yan, *Analyst*, 1993, **118**, 521–527.
37 X. Mao, H. X. Lai, J. N. Li, P. Gao and Z. H. Yan, *Chin. Chem. Lett.*, 2004, **15**, 1315–1318.
38 J. Tursunqulov, N. Qutlimurotova, M. Fayzullayeva, E. Berdimurodov, S. Raximov, Z. Smanova, A. Dadamatov, N. Aliev and A. H.- Bandegharaei, *Int. J. Environ. Anal. Chem.*, 2024, 1–24, DOI: **10.1080/03067319.2024.2333988**, in Press.
39 S. Oszwadowski, R. Lipka and M. Jarosz, *Anal. Chim. Acta*, 1998, **361**, 177–187.
40 R. Purohit and S. Devi, *Talanta*, 1997, **44**, 319–326.
41 W. Simon, *Chimia*, 1990, **44**, 395–398.

42 W. R. Seitz, *CRC Crit. Rev. Anal. Chem.*, 1998, **19**, 135–140.
43 R. F. Alshehri, M. Hemdan, A. O. Babalghith, A. S. Amin and E. R. Darwish, *RSC Adv.*, 2024, **14**, 712–724.
44 L. K. Chau and M. D. Porter, *Anal. Chem.*, 1990, **62**, 1964–1967.
45 I. Oehme, S. Praltes, O. S. Wolfbeis and G. J. Mohr, *Talanta*, 1998, **47**, 595.
46 J. E. Lee and S. S. Saavedra, *Anal. Chim. Acta*, 1994, **285**, 265.
47 A. A. Ensafi and A. Aboutalebi, *Sens. Actuators, B*, 2005, **105**, 479.
48 O. S. Wolfbeis, *Anal. Chem.*, 2002, **74**, 2663–2678.
49 Y. M. Scindia, A. K. Pandey, A. V. R. Reddy and S. B. Manohar, *Anal. Chim. Acta*, 2004, **515**, 311–321.
50 S. Sodaye, R. Tripathi, A. K. Pandey and A. V. R. Reddy, *Anal. Chim. Acta*, 2004, **514**, 159–162.
51 F. Capitan, A. Navalon, E. Manzano, J. L. De-Grancia, L. F. Capitan-Vallvey and J. L. Vilchez, *Analusis*, 1991, **19**, 132–133.
52 F. B. M. Suah, M. Ahmad and L. Y. Heng, *Sens. Actuators, B*, 2014, **201**, 490–495.
53 J. Mendham, R. C. Denney, J. D. Barnes and M. Thomas, *Vogel's Text-Book of Quantitative Chemical Analysis*, Prentice Hall, New York, 6th edn, 2000, pp. 473.
54 H. T. S. Britton, *Hydrogen Ions*, Chapman and Hall, London, 4th edn, 1952.
55 A. S. Amin and M. S. Ibrahim, *Ann. Chim.*, 2001, **91**, 103–110.
56 A. S. Amin and E. H. El-Mossalamy, *J. Trace Microprobe Tech.*, 2003, **21**, 637–648.
57 A. S. Amin, *Anal. Lett.*, 1999, **32**, 1575–1587.
58 A. S. Amin, *Microchem. J.*, 2000, **65**, 261–267.
59 A. S. Amin, *Quim. Anal.*, 2001, **20**, 145–151.
60 A. S. Amin, *Anal. Lett.*, 2001, **34**, 163–176.
61 A. S. Amin, I. M. E. Moustafa and A. El-Sharjawy, *Can. Chem. Trans.*, 2015, **3**, 486–496.
62 C. C. Li and M. S. Kuo, *Anal. Sci.*, 2002, **18**, 607–609.
63 K. Saidi, W. Chaabani and M. Dammak, *RSC Adv.*, 2021, **11**, 30926.
64 M. Ahmad and R. Narayanaswamy, *Sens. Actuators B*, 2002, **81**, 259–266.
65 L. D. Nghiem, P. Mornane, I. D. Potter, J. M. Perera, R. W. Cattrall and S. Kolev, *J. Membr. Sci.*, 2006, **281**, 7–41.
66 K. M. Wygladacz and E. Bakker, *Anal. Chim. Acta*, 2005, **532**, 61–69.
67 C. McDonagh, C. S. Burke and B. D. MacCraith, *Chem. Rev.*, 2008, **108**, 400–422.
68 R. Narayanaswamy and O. S. Wolfbeis, Optical Sensors for Industrial, *Environmental and Diagnostics Applications*, Springer, Berlin, 2004.
69 IUPAC, *Sens. Actuators B*, 1978, **33**, 241–245.
70 K. Sekine and H. Onishi, *Anal. Chim. Acta*, 1972, **62**, 204–206.
71 J. B. Ghasemi and E. Zolfonoun, *Talanta*, 2010, **80**, 1191–1197.
72 S. B. Savvin, *Arsenazo III, Atom Izdat*, Moscow, 1966.
73 H. Bagheri, M. Saber-Tehrani, M. R. Shishehbore and M. Shahvazian, *Prog. Color, Color. Coat.*, 2010, **3**, 58–65.
74 K. Grudpan, M. Utamong and C. G. Taylor, *Anal. Commun.*, 1998, **35**, 107–108.
75 S. Kalyanaraman and T. Fukasawa, *J. Anal. Chem.*, 1983, **55**, 2239–2241.
76 S. G. Nagarkar and M. C. Eshwar, *Microchim. Acta*, 1974, **62**, 797–800.
77 Z. Marczenko and M. Balcerzak, in Separation, preconcentration and spectrophotometry in inorganic analysis, *Analytical Spectroscopy Library*, ed. E. Kloczko, Elsevier, New York, 2000, vol. 10, pp. 474–480.
78 S. Ganesh, P. Velavendan, N. K. Pandey, U. K. Mudali and R. Natarajan, *Int. J. Adv. Pharm., Biol. Chem.*, 2014, **2**, 1–8.
79 S. Kumar, S. Maji and K. Sundararajan, *Appl. Spectrosc.*, 2022, **76**, 635–643.
80 E. Zolfonoun, *Anal. Methods Environ. Chem. J.*, 2020, **3**, 18–24.
81 G. V. Rathaiah and M. C. Eshwar, *Talanta*, 1988, **36**, 502–504.
82 A. Jain, O. Prakash and L. R. Kakkar, *J. Anal. Chem.*, 2010, **65**, 820–824.
83 A. A. A. Sari, A. O. Babalghith, R. El-Sayed and A. S. Amin, *Res. Chem.*, 2024, **7**, 101513.
84 A. S. amin, *J. Taibah Univ. Sci.*, 2015, **9**, 227–236.
85 A. Ringbom, *Chemie*, 1939, **115**, 332–343.
86 S. M. Khopkar, *Basic Concepts of Analytical Chemistry*, New Age International, 1998.
87 J. N. Miller and J. C. Miller, *Statistics and Chemometrics for Analytical Chemistry*, Prentice-Hall, London, 5th edn, 2005.
88 M. L. Firdaus, K. Norisuye, T. Sato, S. Urushihara, Y. Nakagawa, S. Umetani and Y. Sohrin, *Anal. Chim. Acta*, 2007, **583**, 296–302.
89 X. Chang, X. Wang, N. Jiang, Q. He, Y. Zhai, X. Zhu and Z. Hu, *Microchim. Acta*, 2008, **162**, 113–119.
90 B. Cyriac, M. Vali and N. Ojha, *J. Chem. Sci.*, 2020, **132**, 91–101.
91 S. Oszwałdowski and J. Jakubowska, *Talanta*, 2003, **60**, 643–652.